Effects of N doping on photoelectric properties of along different directions of ZnO bulk and nanotube*

Zheng Hong-Mei(郑红梅)[a], Fang Xiao-Yong(房晓勇)[a]†, Cai Li-Xia(蔡丽霞)[a], Yin Ai-Cha(尹爱查)[a], Jin Hai-Bo(金海波)[b], Yu Xiao-Xia(于晓霞)[a], and Cao Mao-Sheng(曹茂盛)[b]‡

[a] *School of Science, Yanshan University, Qinhuangdao* 066004, *China*

[b] *School of Materials Science and Engineering, Beijing Institute of Technology, Beijing* 100081, *China*

(Received 4 April 2014; revised manuscript received 30 June 2014; published online 10 October 2014)

The electronic structures and optical properties of N-doped ZnO bulks and nanotubes are investigated using the first-principles density functional method. The calculated results show that the main optical parameters of ZnO bulks are isotropic (especially in the high frequency region), while ZnO nanotubes exhibit anisotropic optical properties. N doping results show that ZnO bulks and nanotubes present more obvious anisotropies in the low-frequency region. Thereinto, the optical parameters of N-doped ZnO bulks along the [100] direction are greater than those along the [001] direction, while for N-doped nanotubes, the variable quantities of optical parameters along the [100] direction are less than those along the [001] direction. In addition, refractive indexes, electrical conductivities, dielectric constants, and absorption coefficients of ZnO bulks and nanotubes each contain an obvious spectral band in the deep ultraviolet (UV) (100 nm∼ 300 nm). For each of N-doped ZnO bulks and nanotubes, a spectral peak appears in the UV and visible light region, showing that N doping can broaden the application scope of the optical properties of ZnO.

Keywords: ZnO NTs, N-doped ZnO, electronic structure, optical properties, first-principles theory

PACS: 61.46.Fg, 61.72.uj, 73.22.–f, 63.20.dk **DOI:** 10.1088/1674-1056/23/12/126102

1. Introduction

Zinc oxide (ZnO) and its nanostructures which possess novel and unique physical properties have been attracting much attention in various fields such as photoelectric detection,[1–3] hydrogen storage, microwave absorption, nano lasers, sensors, solar cells, spintronic devices, and other fields.[4–12] Because the ZnO is regarded as one of the important materials of next generation electronic devices, much attention has been paid to the research on doped ZnO in recent years. Many researchers have drawn attention to ZnO one-dimensional nanostructure. For example, Pan *et al*. studied the physical model for the exotic ultraviolet photo-conductivity of ZnO nanowire films.[13] Shi *et al*.,[14] Dhara and Giri,[15] and Thomas *et al*.[16] respectively investigated the physical properties, such as force, thermal, optical and electrical properties of Ga-, Al- and Ag-doped ZnO nanowire. In 2009, Sieber *et al*. found the luminescence of the N-doped ZnO nanorods.[17] Wu *et al*. have researched S-, Se-, Te-doped ZnO semiconductors.[18] In addition, some investigations have been reported as regards ZnO nanotubes (NTs). For example, Xu *et al*.,[19] Xing *et al*.[20,21] have successfully synthesized ZnO nanotubes with different wall thickness values and nanobute diameters. The special characteristics of optical spectra of ZnO single-wall nanotubes (SWNTs) have been investigated.[22,23] The calculated results of optical properties of $(n,0)$ ZnO SWNTs studied have revealed that each of the dielectric peaks has a blue shift and the edge of absorption band corresponds to ultraviolet band with the decrease of the nanotubes diameter.[24] While, the absorptions of Ag-doped, Mn-doped, Cd-doped ZnO SWNTs, and Sr-doped ZnO nanotubes have respectively been found and studied, and the phenomenon of a slight red shift was found in Cd-doped ZnO SWNTs, while strong absorptions in the visible-light region of pristine and Sr-doped ZnO nanotubes were observed.[25–28] Feng *et al*. observed that bandgap increases when N atoms are doped into ZnO nanotube and that a red shift appears with the increase of N concentration.[29] Now, the doping of several alkali and alkaline earth metals into sidewall of an armchair ZnO nanotube has been investigated by the density functional theory.[30] These research results greatly promote the progress in studying the optical properties of ZnO nanotubes. So far, N doping has been recognized as one of the most promising solutions to realize p-type ZnO, so that recently many N-doped ZnO nanowires have been reported,[31,32] but there are few research reports about N-doped nanotubes. In addition, varieties of ZnO SWNTs have been widely studied,[19–30,33–35] but the reports of the optical photoelectric properties of N-doped ZnO nanotubes have been particularly rare.

In this paper, nanotubes and N-doped models based on

*Project supported by the State Key Program of the National Natural Science Foundation of China (Grant No. 51132002) and the Natural Science Foundation of Hebei Province, China (Grant No. A2011203026).

†Corresponding author. E-mail: fang@ysu.edu.cn

‡Corresponding author. E-mail: caomaosheng@bit.edu.cn

© 2014 Chinese Physical Society and IOP Publishing Ltd

hexagonal wurtzite ZnO structures are built by Material Studio 5.0 software, and the spectra of band structure, dielectric constants, refractive indexes, absorption coefficients, loss coefficients, and electrical conductivities of ZnO bulks, nanotubes, N-doped ZnO bulks, and nanotubes are calculated using the first principles method. The lattice parameters and the variable quantities of the electron effective mass of ZnO bulks and nanotubes, N-doped ZnO bulks and nanotubes have also been obtained, and the effects of N doping on photoelectric properties of ZnO bulks and nanotubes have been studied comparatively. N doping changes the electronic structures, band gaps and the effective mass values of ZnO bulks and nanotubes. N-doped ZnO shows good photoelectrical properties at low frequency, so it provides an important theoretical basis for the application of zinc oxide in the photoelectric area.

2. Computational method and model

2.1. Computational method

In this paper, the calculations are carried out using the first-principle plane-wave pseudo-potential with Cambridge Serial Total Energy Package (CASTEP) code in Material Studio 5.0 software. Under the condition of *ab initio* method of the plane wavelet pseudo-potential and two-dimensional periodic boundary conditions, the multi-electronic system is expanded with plane wave functions. In order to minimize the number of plane wavelets, the interactions of ion core with valence electrons (O $2s^2 2p^4$, Zn $3d^{10} 4s^2$, N$2s^2 2p^3$) of the atoms are described by the ultrasoft pseudo-potential. In the reciprocal space, the plane-wave cutoff energy is assumed to be 380 eV, and the generalized gradient approximation (GGA) and Perdew and Wang 91 (PW91) are employed for the exchange–correlation potential. The sampling k-points are set to be $1\times1\times4$ in Brillouin zone of ZnO according to the Monkhorst-pack scheme. The ground state energy is calculated using Pulay density mixed method, and the self-consistent field is set to be 1×10^{-6} eV/atom.

The structure is optimized with the Broyden–Fletcher–Goldfarb–Shanno (BFGS) method and four optimization parameters are as follows: 1) the convergence standard of the individual-atom energy is 1.0×10^{-5} eV, 2) the convergence standard of interaction between electrons is 0.3 eV/nm, 3) the convergence standard for maximum shift of atom is 1.0×10^{-4} nm, and 4) the convergence standard of crystal internal stress is 0.05 GPa. The optimization for four parameters is carried out simultaneously and the indication of the completeness is that four parameters all meet the convergence standard.

2.2. Structural model

ZnO has a variety of crystal structures, including the hexagonal wurtzite ZnO which belongs to $P6_3mc$ space group, and its symmetry is C_{6v}^4, The hexagonal close packing of zinc and oxygen reversely nest along the c axis. Zinc atoms are located on the tetrahedral gap formed by four adjacent oxygen atoms. The arrangement of oxygen atoms is similar to zinc's, figure 1(a) is the ZnO supercell whose structure is $3\times3\times1$ making up of 36 atoms.

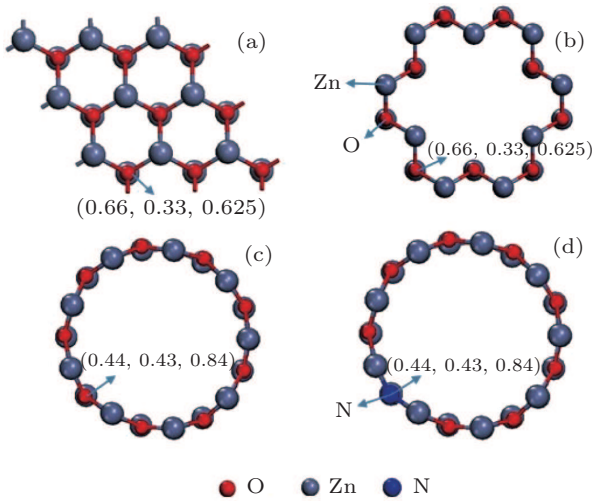


Fig. 1. (color online) (a) supercell structure with the same atomic number as ZnO NTs, (b) serrated ZnO NTs before optimization, (c) optimized circular ZnO NTs, and (d) optimized circular N-doped ZnO NTs. Positions in this figure are the coordinates of the substituted oxygen atom.

The single-walled nanotubes which remove superfluous atoms beside one layer from the hexagonal wurtzite ZnO can be obtained. It periodically arranges along the [001] direction, and the least positive period contains 36 atoms, in which there are 18 zinc and 18 oxygen atoms as shown in Fig. 1(b). The optimized structure of ZnO nanotubes is shown in Fig. 1(c). N-doped ZnO supercell and nanotubes are obtained through substituting nitrogen atom for the positions (0.66, 0.33, 0.625) of oxygen atom. The optimized structure of N-doped ZnO nanotubes is shown in Fig. 1(d).

3. Results and discussion

3.1. Crystal structure

In the reciprocal space, geometry optimization, which is achieved using the BFGS algorithm, makes the structure more stable, and the variable quantity of system in the total energy is no more than 10 μeV/atom. After the geometry optimization, the accuracies of self-consistence and the system energies of ZnO bulks and ZnO nanotubes with the same N-doped consistence each have a better convergence, and these are less than the standard. Part of the calculation results are shown in Table 1.

Table 1. Lattice parameters of ZnO and N-doped ZnO.

	ZnO				N-doped ZnO			
	Lattice (a/c)/Å	Bond length O–Zn/Å	Bond angle ∠ZnOZn/(°)	Diameter D/Å	Lattice (a/c)/Å	Bond length O–Zn/Å	Bond angle ∠ZnOZn/(°)	Diameter D/Å
Bulk	3.283	2.001	108.653	∞	3.279	1.949	109.147	∞
	5.298	2.009	110.778		5.311	1.955	111.036	
Nanotube	3.314	1.905	114. 893	9.611	3.331	1.881	114.576	9.560
	5.663	1.907	118. 435		5.649	1.889	118.657	

As illustrated in Table 1, the bond lengths of O(N)–Zn decrease no matter whether the ZnO doped with N. Because the bond angle of N-doped ZnO NT is increased by about 6°, the lattice constants of nanotube are bigger than those of bulk. N atom destroys the original state of equilibrium of ZnO. It is perceived that the influences of N doping on the lattice structure of bulks and nanotubes are significantly different, as listed below.

(i) The bond lengths of bulks decrease and the bond angles increase, while both the bond lengths and bond angles of nanotubes decrease;

(ii) Owing to the effect of quantum size, the variables of bond length and bond angle of bulks are more obvious than those of nanotubes;

(iii) Doping causes the diameter of nanotubes to decrease by about 0.051 Å, mainly due to the bond length and bond angle decreasing;

(iv) The combined action of bond length and bond angle determines the change of lattice constant. Doping allows lattice constant a of bulk to reduce and c to increase, but nanotubes have a contrary scenario. Lattice constant has an effect on the effective mass values of electrons and holes, and the influence is shown in the following subsection. This maybe the main influences on the change of band structure and the frequency shift of dielectric function.

3.2. Electronic property

The band structures of bulks and ZnO nanotubes are shown in Fig. 2. The band gap of ZnO bulks is less than

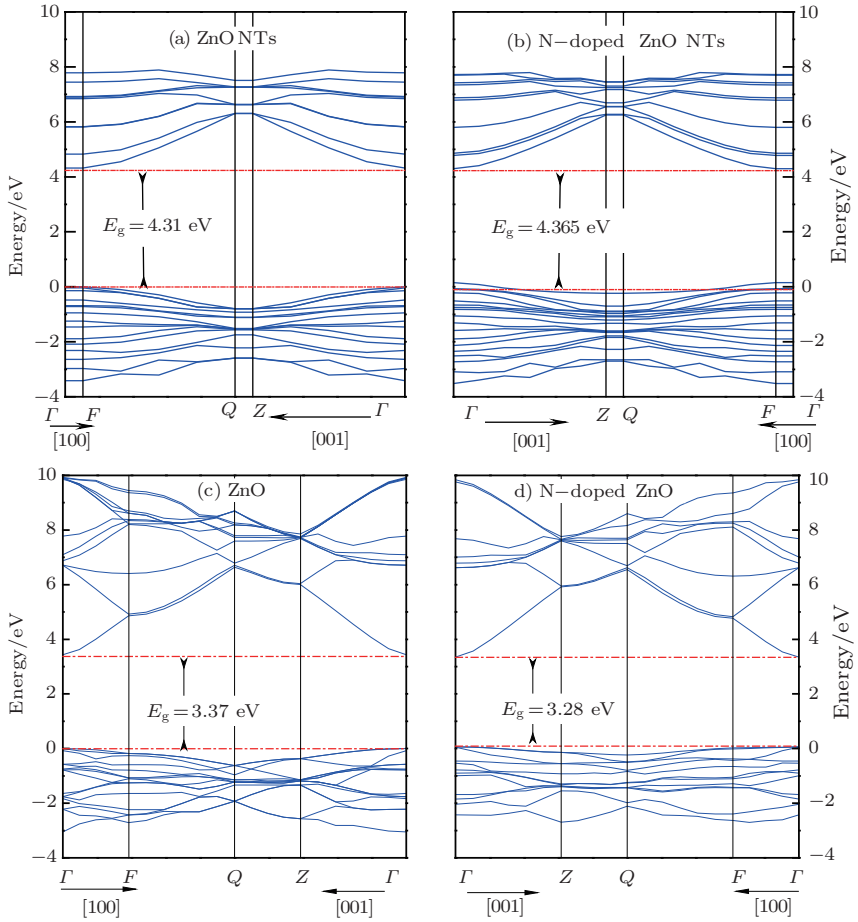


Fig. 2. (color online) Band structures of ((a) and (c)) the pure and ((b) and (d)) N-doped ZnO bulk and NTs. The scissors operator is at 2.628 eV.

3.37 eV from the experimental result, owing to the fact that the correlation interaction between excited electrons in calculating model has been underestimated. On account of overestimating the energy of Zn-3d, the Zn-3d and O-2p violently hybridize and bandwidth of valence band increases, therefore the band-gap decreases. In consequence, the scissors operator is revised in Fig. 2.

As shown in Fig. 2, the top of valence band (VBM) and the bottom of conduction band (CBM) of ZnO nanotubes and bulks are in the center of the Brillouin zone (Γ), and they are direct band-gap semiconductor. The direct band gap properties of ZnO make them good candidates for applications in optoelectronic nanodevices. It is known that the effective mass values of electrons and holes can be calculated by using the formula of the solids physics:

$$\left(\frac{1}{m^*}\right)_{ij} = \frac{1}{\hbar^2}\frac{\partial^2 E}{\partial k_j \partial k_i}, \quad (i,j = x,y,z), \tag{1}$$

and the results are listed in Table 2.

Electronic density of states (DOS) of ZnO nanotube and N-doped nanotube are illustrated in Fig. 3. The VBs of pure and N-doped ZnO nanotubes are composed of the bottom of VB contributed by Zn-3d, the VBM is contributed by O-2p, and in -17 eV the VB is provided by O-2s. Because of N substituting for O, it introduces two belts of impurity: one is on the VBM provided by N-2p, and the other is located in -13 eV and provided by N-2s. As shown in Fig. 3, the insets respectively show the partly enlarged CB, and the CB of nanotubes is mainly provided by the 4s orbits of Zn and Zn-3p. At the upper portion of VB, the VB contributed by Zn-3d changes more gently and the peak of state density of O-2p is sharp, owing to the full shell structure of orbital of Zn-3d, thus the holes of VB hold large effective mass.

DOSs of pure and N-doped ZnO bulks have similar performances to those shown in Fig. 3, except for two impurity belts.

Compared with bulks, band structure in Fig. 2 shows that the band gaps of nanotubes all increase. It is perceived that the influences of N doping on the band structure of bulks and nanotubes are significantly different as described below.

i) For ZnO bulks, N doping brings degenerate impurity band (bandwidth is 0.064 eV) at the VBM, so the impurity band and VB form a new VB, which induces the band gap to decrease;

ii) For ZnO nanotubes, an impurity energy level is newly added to the VBM, which derives from 2p orbital of N and is close to the VBM (about is 0.219 eV) due to N doping, so that impurity energy level can serve as a good acceptor impurity. ZnO bulks are of 3d periodic structures, and the number of N atoms participating in the calculation are far more than that of one-dimensional periodic structure, therefore there is only impurity band level in Fig. 2(b). While a large number of impurity levels form an impurity band in Fig. 2(d);

iii) Because of approximating parabolic shape, the CB is a quasi-sp energy band;

iv) The increment of the CB of nanotubes is less than that of ZnO bulk, while that of VB shows an opposite scenario. That indicates that the electronic effective mass of nanotube is greater than that of the bulk, while that of hole exhibits an opposite scenario, and the computation results are shown in Table 2.

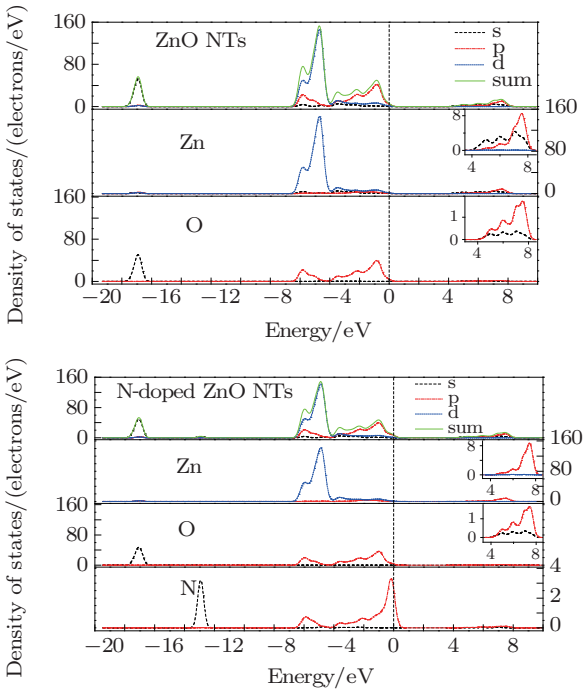


Fig. 3. (color online) Electronic densities of states of (a) pure ZnO NTs and (b) N-doped ZnO NTs.

Table 2. Band structure parameters of ZnO and N-doped ZnO.

	ZnO			N-doped ZnO			
	Band gap E_g/eV	Effective mass		Band gap E_g/eV	Effective mass		Impurity band/eV
		$m_e(m_0)$	$m_h(m_0)$		$m_e(m_0)$	$m_h(m_0)$	
Bulk	3.37	*a*-0.69 *c*-0.71	*a*-5.46 *c*-6.06	3.28	*a*-0.74 *c*-0.27	*a*-7.70 *c*-10.6	0.064
Nanotube	4.31	*a*-2.19 *c*-0.86	*a*-4.90 *c*-2.64	4.37	*a*-1.89 *c*-0.82	*a*-5.90 *c*-3.46	0.219

3.3. Photoelectric properties

The calculated results of dielectric functions, loss coefficients, refractive indexes, conductivities, absorption coefficients of pure and N-doped ZnO bulks and nanotubes are demonstrated in Figs. 4–7.

From Fig. 4 it follows that

(I) The variable quantities of dielectric constants of ZnO bulks along the [100] direction and [001] direction are small, so that they hold isotropic dielectric properties. While dielectric constants of ZnO nanotubes along the [001] direction (both real part and imaginary part) are greater than along [100] direction, dielectric properties are anisotropic;

(II) N-doping has a great influence on dielectric constant of ZnO bulk along the [100] direction, while a less influence along the [001] direction. Inversely, N-doping makes greater influence on dielectric constant of ZnO nanotubes along the [001] direction (both real and imaginary part) than along the [100] direction;

(III) Wing to N-doping, peaks appear at the low frequencies of ZnO bulks and nanotubes respectively, which broadens the application scope. The peak follows Lorentz model which is given as follows:[36]

$$\varepsilon = 1 + \frac{e^2 N}{m^* \varepsilon_0}\left[\frac{(\omega_0^2 - \omega^2)}{(\omega_0^2 - \omega^2)^2 + (\omega/\tau)^2} + \mathrm{i}\frac{\omega/\tau}{(\omega_0^2 - \omega^2)^2 + (\omega/\tau)^2}\right]. \quad (2)$$

It illustrates that the peaks derive from the free electron oscillations provided by impurities band belt (or impurity energy level).

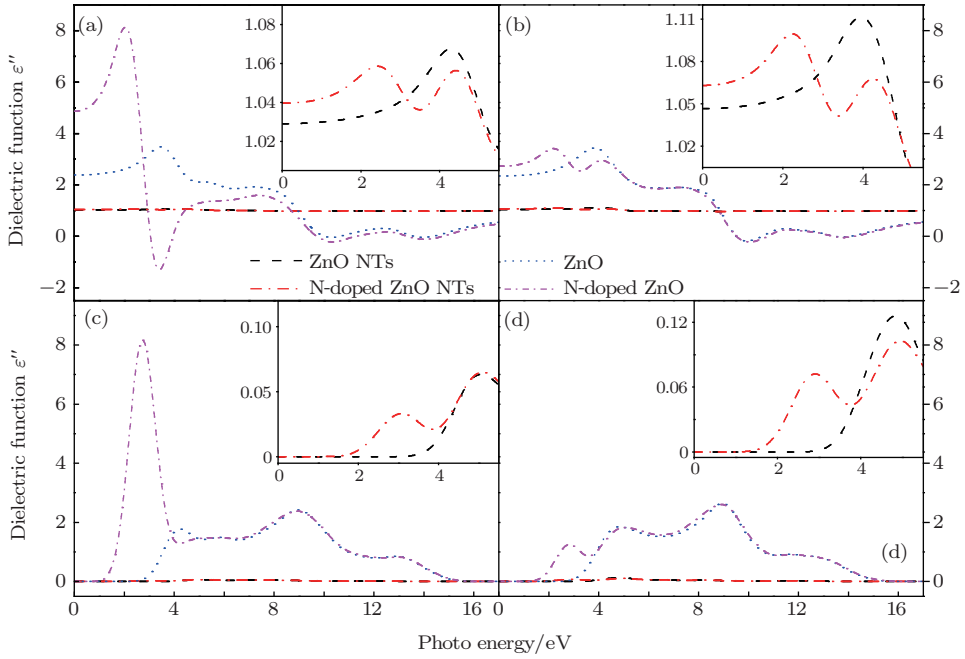


Fig. 4. (color online) Dielectric constants of pure and N-doped ZnO bulks and NTs ((a) and (c)) along the [100] direction, and ((b) and (d)) along the [001] direction. The insets show the partial enlargements.

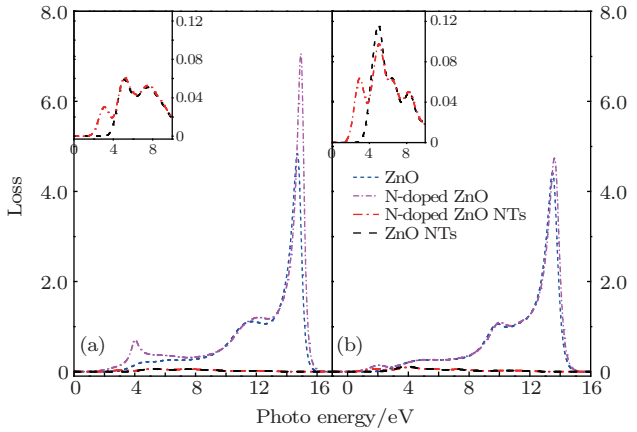


Fig. 5. (color online) Loss coefficients of pure and N-doped ZnO bulks and NTs (a) along the [100] direction and (b) along [001] direction. The insets show the partial enlargements of the curves for the pure and N-doped ZnO NTs.

For completeness, the spectra of the dielectric loss function of pure and N-doped ZnO bulks and nanotubes along different directions can also be given as shown in Fig. 5. For ZnO nanotubes, N-doping exerts a greater influence along the [001] direction than along the [100] direction, and leads to peaks appearing in a low frequency range (from 3 eV to 4 eV) of ZnO bulks and nanotubes respectively.

In Figs. 6 and 7, the refractive indexes, photoconductions, and absorption coefficients of pure and N-doped ZnO bulks and nanotubes along the [100] direction and the [001] direction can be calculated from the relationship between dielectric constants and refractive index, and that between extinction coefficient κ and absorption coefficient α:[37]

$$n^2 - k^2 = \varepsilon_1, \quad (3)$$

$$2n\kappa = \varepsilon_2, \tag{4}$$

$$\alpha = \frac{2\omega\kappa}{c} \quad . \tag{5}$$

The spectral characteristics are similar to the dielectric constant:

I) The variations of the refractive indexes, extinction coefficients, loss coefficients, absorption coefficients, and photoconductions along the [100] direction and the [001] direction of ZnO bulks are small, namely these parameters are isotropic. While the parameters along the [001] direction are greater than along the [100] direction, so the above optical parameters of ZnO nanotubes exhibit anisotropic properties;

II) N doping exerts a great influence on the optical parameters of ZnO bulk along the [100] direction but less along the [001] direction. On the other hand, N doping has a greater effect on these optical parameters along [001] direction than along the [100] direction in ZnO nanotubes;

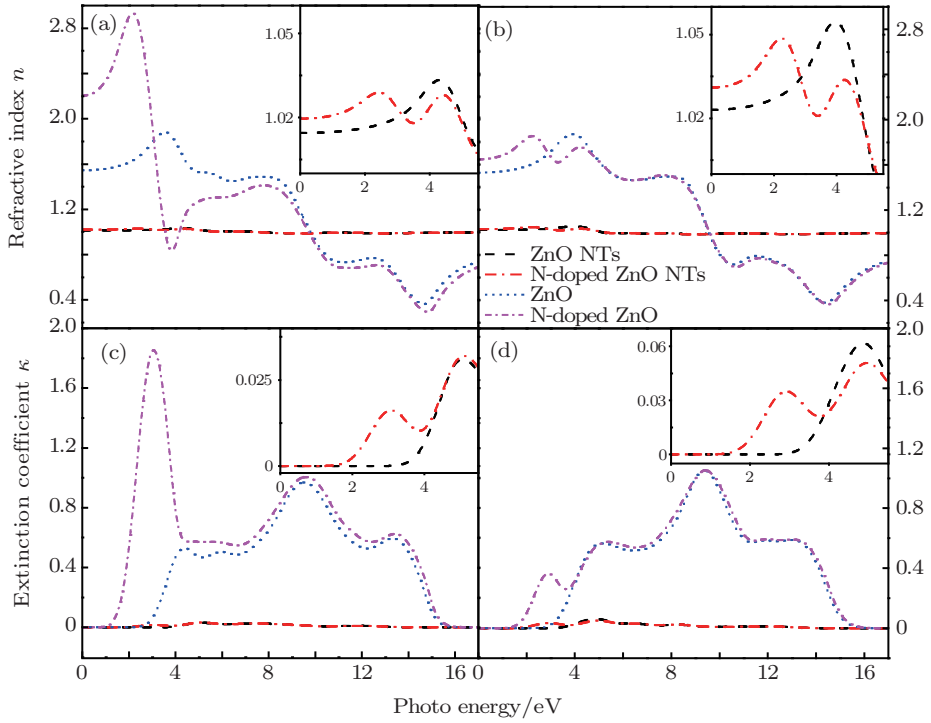


Fig. 6. (color online) Refractive indexes and extinction coefficients of pure and N-doped ZnO bulks and NTs ((a) and (c)) along the [100] direction and ((b) and (d)) along the [001] direction. The insets show the partial enlargements.

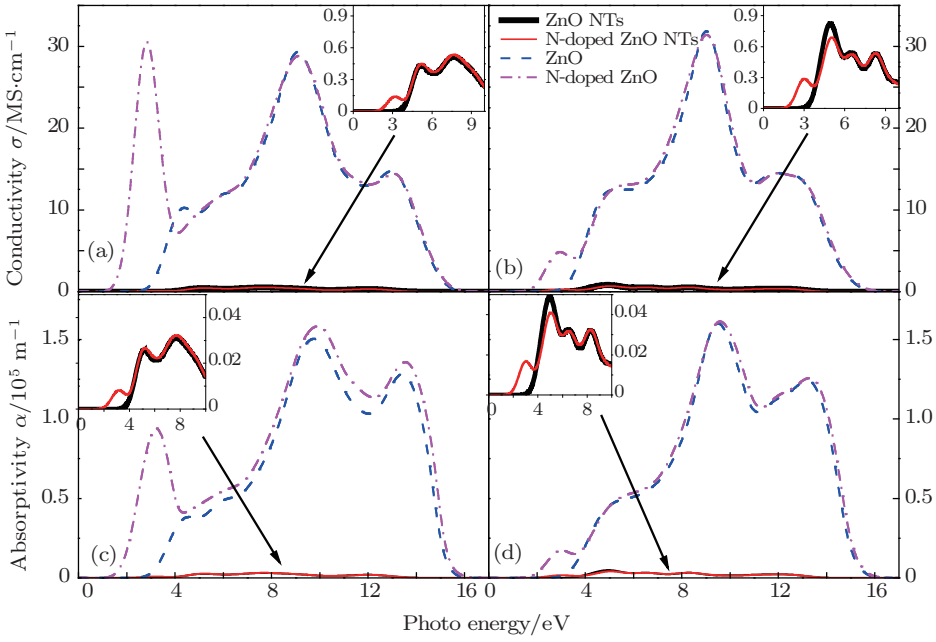


Fig. 7. (color online) Absorption coefficients and conductivity coefficients of pure and N-doped ZnO bulks and NTs ((a) and (c)) along the [100] direction and ((b) and (d)) along the [001] direction. The insets show the partial enlargements of the curves for the pure and N-doped ZnO NTs.

III) For ZnO bulks and nanotubes, the waveforms of the absorption coefficients, and conductivities are similar. In addition, these spectra have peaks appearing in a 4 eV–14 eV (about 89 nm–310 nm) ultraviolet range. While strong absorption (and conductivity) peaks which come from the increased conductivities of N-doped ZnO bulk and nanotube turns up at 2 eV–4 eV (about 310 nm–62 0nm) ranging from UV to visible light. Like dielectric function performance analysis, the peak is derived from the impurity level. The absorption and conductivity spectra of ZnO are broaden from deep UV (89 nm) region to visible light (620 nm) region. Light-absorption and conductivity spectrum edges of the N-doped ZnO are red-shifted, exactly the same as the properties of nanoparticles[38] and N-doped ZnO thin films.[39]

4. Conclusions

In this paper, the band structures, refractive indexes, absorption coefficients, loss coefficients, electrical conductivities, and dielectric constants of pure and N-doped ZnO bulks and nanotubes are calculated by MS software CASTEP module. The lattice parameters and the changes of the electron effective mass of pure and N-doped ZnO bulks and nanotubes are also obtained, and the effects of N doping on photoelectric properties of ZnO bulks and nanotubes are comparatively studied. The calculated results show that the main optical parameters of ZnO bulks are isotropic (especially in a high frequency region), while ZnO nanotubes exhibit anisotropic optical properties. N doping results show that N-doped ZnO bulks and nanotubes present more obvious anisotropic properties in a low-frequency region. Thereinto, the optical parameters of N-doped ZnO bulks along the [100] direction are greater than along the [001] direction, while for N-doped nanotubes, the variable quantities of optical parameters along the [100] direction are less than along the [001] direction. In addition, according to the calculated results of optical properties and the formula of $\lambda = 1240/E$, it is found that the N doping causes the absorption and conductivity spectra of ZnO to shift from deep UV (89 nm) region to visible light (620 nm) region, indicating that the N doping can broaden photovoltaic application fields of ZnO.

References

[1] van Vugt L K, Ruhle S, Ravindran P, Gerritsen H C, Kuipers L and Vanmaekelbergh D 2006 *Phys. Rev. Lett.* **97** 147401
[2] Wang R P, Xu G and Jin P 2004 *Phys. Rev. B* **69** 113303
[3] Grabowska J, Meaney A, Nanda K K, Mosnier J P, Henry M O, Duclere J R and McGlynn E 2005 *Phys. Rev. B* **71** 115439
[4] Koukli N 2008 *Adv. Mater.* **20** 2190
[5] Pan H, Luo J Z, Sun H, Feng Y P, Poh C K and Lin J Y 2006 *Nanotechnology* **17** 2963
[6] MacDonald A H, Schiffer P and Samarth N 2005 *Nat. Mater.* **4** 195
[7] Huang M H, Mao S, Feick H, Yan Y H, Wu V Y, Kind H, Weber E, Russo R and Yang P 2001 *Science* **292** 1897
[8] Nomura K, Ohta H, Ueda K, Kamiya T, Hirano M and Hosono H 2003 *Science* **300** 1269
[9] Suchea M, Christoulakis S, Moschovis K, Katsarakis N and Kiriakidis G 2006 *Thin Solid Films* **515** 551
[10] Fang X Y, Shi X L, Cao M S and Yuan J 2008 *J. Appl. Phys.* **104** 096101
[11] Fang X Y, Cao M S, Shi X L, Hou Z L, Song W L and Yuan J 2010 *J. Appl. Phys.* **107** 054304
[12] Gong W, Xu Z, Zhao S L, Liu X D, Fan X, Yang Q Q and Kong C 2013 *Chin. Phys. B* **22** 128402
[13] Pan Y W, Ren S T, Qu S L and Wang Q 2013 *Chin. Phys. B* **22** 118102
[14] Shi L H, Chen J, Zhang G and Li B W 2012 *Phys. Lett. A* **376** 978
[15] Dhara S and Giri P K 2012 *Chem. Phys. Lett.* **541** 39
[16] Thomas M A, Sun W W and Cui J B 2012 *J. Phys. Chem. C* **116** 6383
[17] Sieber B, Liu H Q, Piret G, Laureyns J, Roussel P, Gelloz B, Szunerits S and Boukherroub R 2009 *J. Phys. Chem. C* **113** 13646
[18] Wu K P, Gu S L, Ye J D, Tang K, Zhu S M, Zhou M R, Huang Y R, Zhang R and Zheng Y D 2013 *Chin. Phys. B* **22** 107103
[19] Xu W Z, Ye Z Z, Ma D W, Lu H M, Zhu L P, Zhao B H, Yang X D and Xu Z Y 2005 *Appl. Phys. Lett.* **87** 093110
[20] Xing Y J, Xi Z H, Zhang X D, Song J H, Wang R M, Xu J, Xue Z Q and Yu D P 2004 *Solid State Commun.* **129** 671
[21] Xing Y J, Xi Z H, Xue Z Q, Zhang X D, Song J H, Wang R M, Xu J, Song Y, Zhang S L and Yu D P 2003 *Appl. Phys. Lett.* **83** 1689
[22] Elizondo S L and Mintmire J W 2007 *J. Phys. Chem. C* **111** 17821
[23] Yang Y R, Yan X H, Guo Z H and Deng Y X 2008 *Chin. Phys. B* **17** 3433
[24] Dong J T, Zhang F C, Zhang W H and Zhang Z Y 2013 *Sci. China: Phys. Mech. Astron.* **56** 706
[25] Chai G L, Lin C S, Wang J Y, Zhang M Y, Wei J and Cheng W D 2011 *J. Phys. Chem. C* **115** 2907
[26] Moradian R and Shahrokhi M 2012 *Physica E* **44** 1760
[27] Wang S F, Zhang J M, Chen L Y and Xu K W 2012 *J. Supercond. Nov. Magn.* **25** 2457
[28] Moradian R and Shahrokhi M 2013 *J. Phys. Chem. Solids* **74** 1063
[29] Feng X Y, Zhang C W, Xu X J and Wang P J 2013 *Nanoscale Res. Lett.* **8** 365
[30] Peyghan A A and Noei M 2014 *Physica B* **432** 105
[31] Gao J Y, Zhang X Z, Sun Y H, Zhao Q and Yu D P 2010 *Nanotechnology* **21** 245703
[32] Xu H, Rosa A L, Frauenheim T and Zhang P Q 2010 *Phys. Status Solidi B* **247** 2195
[33] Wang F Z, Liu B, Zha Z J and Yuan S C 2009 *Physica E* **41** 879
[34] He A L, Wang X Q, Fan Y Q and Feng Y P 2010 *J. Appl. Phys.* **108** 084308
[35] Song D M and Li J C 2012 *Comput. Mater. Sci.* **65** 175
[36] Zhou Y, Wang K, Fang X Y, Hou Z L, Jin H B and Cao M S 2012 *Chin. Phys. Lett.* **29** 077102
[37] Feng G Y, Fang X Y, Wang J J, Zhou Y, Lu R, Yuan J and Cao M S 2010 *Physica B* **405** 2625
[38] Sun S B, Chang X T, Li X J and Li Z J 2013 *Ceram. Int.* **39** 5197
[39] Nian H, Hahn S H, Koo K K, Shin E W and Kim E J 2009 *Mater. Lett.* **63** 2246